Superconducting quantum interferometer in a magnetic field

G. F. Zharkov and A. D. Zaikin

P. N. Lebedev Physics Institute, USSR Academy of Sciences
(Submitted 2 July 1979)
Zh. Eksp. Teor. Fiz. **78**, 206–220 (January 1980)

We develop the theory of a superconducting quantum interferometer in an external magnetic field H_c with account taken of the finite geometrical dimensions of the system (L_1, L_2—widths of the tunnel junctions, σ—inside area of the interferometer ring). Exact equations that describe the behavior of an interferometer with finite dimensions are formulated. The problem is solved analytically in the limiting case of a strong external field ($H_e \gg 1$). Plots are constructed of the maximum stationary current I_{max} through the interferometer as a function of the external field H_e at different values of L_1, L_2, and σ. The magnetic field inside the interferometer H_0 is determined as a function of the external magnetic field H_e in the presence of a transport current I through the interferometer. In the limiting case of point junctions ($L_1 = L_2 \ll 1$), the results obtained in the present paper are compared with the corresponding results of other studies.

PACS numbers: 85.25. + k

1. Superconducting quantum interferometers are widely used in a variety of physical experiments and other practical applications (see, e.g., Refs. 1–4), so that an analysis of the operation of such devices is of great importance. In the static regime, greatest interest attaches to the dependence of the maximum transport current through the interferometer on the external field. The resultant characteristic interference relations make it possible to determine with high accuracy the external field, and this finds important applications in a number of cases. The experimentally observed interference curves vary greatly, and it is not always clear which factors cause the differences between them. There are quite a few published theoretical attempts to describe the experimentally observed relations (see the reviews[1-4]). Most papers, however, are restricted to the case of point junctions, and the description makes use of phenomenological parameters of the self-inductance of the interferometer, which take qualitatively into account the presence of screening currents in the system. This leaves unclear the manner in which these coefficients are connected with the geometrical parameters of the system. We develop below a theory that determines the corresponding relations and makes it possible to take into account the influence of the finite geometric dimensions of the interferometer on the critical current.

We consider in the present paper the case of the so-called double quantum interferometer,[5,6] which is most frequently used in practice for precision measurements of a magnetic field. The physical operating principles of this instrument are described in a number of monographs and reviews.[1-4] We formulate below exact equations that describe the behavior of a double interferometer with finite geometrical dimensions in an external field (cf. the analogous problem for a single ring interferometer, considered in Ref. 7). The obtained exact equations are solved in the limiting case of a strong external field ($H_e \gg 1$), and a formula is obtained for the maximum stationary current through the finite-dimension interferometer as a function of the external field. In addition, we determine the law governing the variation of the magnetic field inside the in-

terferometer H_0 as a function of the external magnetic field H_e in the presence of transport current I through the interferometer. The results are illustrated by a number of plots. In the limiting case of junctions of small width ($L_{1,2} \ll 1$), the results obtained in this paper are compared with the equations known from the literature.

2. We choose the system shown in Fig. 1 as the model of the double interferometer. Here $H_{L1} = H_e - H_I$, $H_{L2} = H_e + H_I$, H_e is the external homogeneous magnetic field, H_I is the field of the total transport current I flowing through the interferometer; L_1 and L_2 are the widths of the tunnel junctions and σ is the area of the internal opening (ring) of the interferometer. It is assumed that the external magnetic field H_e is directed along the z axis (perpendicular to the plane of the figure) and that the entire system is infinitely long in the z direction (cylinder). This model is frequently used to study real interferometers and reflects their properties to a certain degree.

We assume, as usual, that the distributions of the fields $H(x)$ and of the currents in the junctions L_1 and L_2 are described by the following differential equations (in dimensionless units):[1)]

$$d^2\varphi_1/dx_1^2 = \sin\varphi_1, \quad d^2\varphi_2/dx_2^2 = \sin\varphi_2;$$
$$H(x_1) = d\varphi_1/dx_1 \quad (0 \leqslant x_1 \leqslant L_1),$$
$$H(x_2) = d\varphi_2/dx_2 \quad (0 \leqslant x_2 \leqslant L_2), \tag{1}$$

where φ_1 and φ_2 are the differences of the phases of the order parameter at the junctions L_1 and L_2. In view of the cylindrical symmetry, the quantities φ_1 and φ_2 depend only on the radial coordinates x_1 and x_2. The coordinate axes x_1 and x_2 lie in the plane of the junctions and are directed along the radius from the inner cavity σ to the outside. It is assumed in Eqs. (1) that the densities of the critical currents of the junctions j_{c1} and j_{c2} are equal and that the junctions differ only in width.

For each of the equations in (1) we can easily write a first integral in the form

$$x = \frac{1}{2} \int_{\varphi_0}^{\varphi(x)} \left\{ \sin^2 \frac{y}{2} + C \right\}^{-1/2} dy, \tag{2}$$
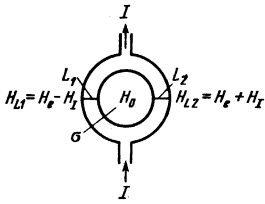
FIG. 1. Schematic diagram of double interferometer.

where $\varphi_0 = \varphi(0)$ and C is an arbitrary constant. The integral (2) yields an explicit expression for the solutions of Eqs. (1), which can be expressed in terms of Jacobi elliptic functions. Using (2), we obtain the relations (cf., e.g., Refs. 7–12)

$$L_1 = \frac{1}{2} \int_{\varphi_{01}}^{\varphi_{L1}} \frac{dy}{R_1(y)}, \quad L_2 = \frac{1}{2} \int_{\varphi_{02}}^{\varphi_{L2}} \frac{dy}{R_2(y)},$$

$$R_{1,2}(y) = \left(\frac{H_0^2}{4} + \sin^2\frac{y}{2} - \sin^2\frac{\varphi_{0\,1,2}}{2} \right)^{1/2}. \tag{3}$$

Here φ_{01} and φ_{02} are the phase differences on the junctions L_1 and L_2 respectively at the points $x_1 = 0$ and $x_2 = 0$, lying on the inner surface of the cavity σ; φ_{L1} and φ_{L2} are the values of the phase difference on the outer surface (i.e., at the points $x_1 = L_1$ and $x_2 = L_2$).

It is easily seen that in addition relations (2) it is necessary to satisfy the equations (cf. Refs. 7–12)

$$\sin^2\frac{\varphi_{L1}}{2} - \sin^2\frac{\varphi_{01}}{2} = \frac{H_{L1}^2 - H_0^2}{4},$$

$$\sin^2\frac{\varphi_{L2}}{2} - \sin^2\frac{\varphi_{02}}{2} = \frac{H_{L2}^2 - H_0^2}{4}, \tag{4}$$

which follow from the boundary conditions to Eqs. (1), namely

$$\frac{d\varphi_1}{dx_1}\Big|_{x_1=0} = \frac{d\varphi_2}{dx_2}\Big|_{x_2=0} = H_0,$$

$$\frac{d\varphi_1}{dx_1}\Big|_{x_1=L_1} = H_{L1}, \quad \frac{d\varphi_2}{dx_2}\Big|_{x_2=L_2} = H_{L2}. \tag{5}$$

In addition to the foregoing, it is necessary to satisfy also the relation

$$\varphi_{01} + \varphi_{02} = \sigma H_0, \tag{6}$$

which is an obvious generalization of the corresponding equation $(\varphi_0 = \sigma H_0)$ used by us earlier[7] for a single ring interferometer.[2] Sometimes there is added to the left-hand side of (6) a term of the type $2\pi n$ (n is an integer), connected with the fact that the phase is determined accurate to such an inessential term. We normalize the phase shifts by the condition that in the absence of fields and currents $(H_0 = H_e = I = 0)$ the phase differences become equal to 0, (i.e., $n = 0$). The condition (6) enables us to connect the jumps of the phases on the junctions directly with a physically observed quantity—the total magnetic flux inside the system.

The group of equations (3)–(6) makes it possible to find the values of the "initial" phases φ_{01} and φ_{02} as functions of the geometric parameters L_1, L_2, and σ at given values of H_e and H_I. This determines simultaneously also the value of the field H_0 that is established

inside the interferometer. Knowledge of the "initial" values φ_0 and of the derivatives $d\varphi/dx|_{x=0} = H_0$ makes it possible to determine uniquely the solutions of the differential equations (1) and obtain the configuration of the fields $H(x) = d\varphi/dx$ and of the currents $j(x) = \sin\varphi(x)$ in both junctions (L_1 and L_2). As a result we obtain a complete description of the behavior of the system under consideration.

The exact solution of Eqs. (3)–(6) entails rather cumbersome numerical calculations of the elliptic integrals in (3); examples of calculations of this kind are given in Refs. 7–11. We confine ourselves below to the limiting case of strong fields ($H_e \gg 1$, cf. Refs. 7 and 12), when Eqs. (3) are degenerate and the problem becomes simpler. We note, incidentally, that a field of even a few gausses is strong in terms of the dimensionless units employed here, so that a condition $H_e \gg 1$ covers a rather wide range of fields. In addition, the obtained formulas in the case point junctions ($L_{1,2} \ll 1$) are valid in arbitrary fields.

3. Thus, let the external field be strong: $H_e \gg 1$. Obviously, in this case the internal field H_0 is also strong: $H_0 \gg 1$. The integral equations (3) degenerate in this case to the simple equalities

$$\varphi_{L1} = \varphi_{01} + L_1 H_0, \quad \varphi_{L2} = \varphi_{02} + L_2 H_0. \tag{7}$$

Equations (4) at $H_0 \gg 1$ can be rewritten with allowance for (7) in the form

$$\frac{H_{L1} - H_0}{2} H_0 = \sin\left(\frac{L_1 H_0}{2}\right) \sin\left(\varphi_{01} + \frac{L_1 H_0}{2}\right).$$

$$\frac{H_{L2} - H_0}{2} H_0 = \sin\left(\frac{L_2 H_0}{2}\right) \sin\left(\varphi_{02} + \frac{L_2 H_0}{2}\right). \tag{8}$$

Eliminating the quantity φ_{02} with the aid of (6) and then eliminating from (8) the quantity $\varphi_{01} + L_1 H_0/2$, we arrive at the following fundamental equation:

$$\left(\frac{H_{L1} - H_0}{s_1}\right)^2 + \left(\frac{H_{L2} - H_0}{s_2}\right)^2 + 2\frac{(H_{L1} - H_0)(H_{L2} - H_0)}{s_1 s_2}\cos \Sigma H_0 = \sin^2 \Sigma H_0. \tag{9}$$

where

$$s_1 = \frac{2}{H_0}\sin\frac{L_1 H_0}{2}, \quad s_2 = \frac{2}{H_0}\sin\frac{L_2 H_0}{2},$$

$$\Sigma = \sigma + (L_1 + L_2)/2. \tag{10}$$

Equation (9) enables us to find the unknown H_0 as a function of the parameters of the problem ($L_1, L_2, \sigma, H_{L1}, H_{L2}$). This equation has a complicated transcendental form with respect to the variable H_0, and we shall therefore solve it relative to the quantity H_I, which enters in Eq. (9) quadratically via the obvious relations

$$H_{L1} = H_e - H_I, \quad H_{L2} = H_e + H_I. \tag{11}$$

Solving the corresponding quadratic equation for H_I, we get from (9)

$$H_I = \frac{(H_e - H_0)(s_2^2 - s_1^2) \pm R}{s_1^2 + s_2^2 - 2s_1 s_2 \cos \Sigma H_0}, \tag{12}$$

where

$$R = \{s_1^2 + s_2^2 - 2s_1 s_2 \cos \Sigma H_0 - 4(H_e - H_0)^2\}^{1/2}|s_1 s_2 \sin \Sigma H_0|. \tag{13}$$

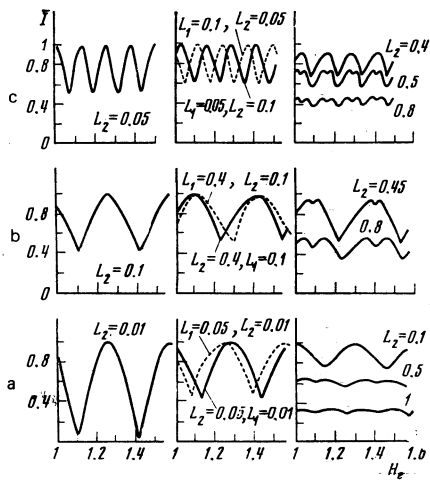FIG. 2. Plot of $\overline{I}=I_{max}/(L_1+L_2)$ against H_e at $H_e \gtrsim 1$: a—σ $=20, L_1=0.01$; b—$\sigma=20, L_1=0.1$; c—$\sigma=50, L_1=0.05$. For small L_1 and L_2 the dependence is periodic up to fields $H_e \sim 1/L_{1,2}$. With increasing field, characteristic interference curves appear (see Fig. 3).

If we assume that $H_I \geq 0$ and are interested only in the maximum current, then we must choose the positive sign in front of the radical in (12).

The values $J_{max}=2H_{Imax}$, obtained from (12) as functions of H_e, are plotted in Figs. 2 and 3 for several values of L_1, L_2, and σ. The character of the transformation of the I_{max} curves when the parameters of the problems are changed is clear from the figures. In the case of broad junctions, as seen from Fig. 3, effects connected with the widths of the junctions $L_{1,2}$ come into play when the field is increased, and interference dependences due to the entry of flux quanta into the interiors of the individual junctions (the minima and maxima of the envelopes of the curves in Fig. 3) begin to manifest themselves against the background of the shallow minima and maxima due to the entry of an integer number of flux quanta into the interferometer ring. With increasing field, the amplitude of the oscillations of the envelope tends to zero like $1/H_e$. We note also the appearance of a nonlinear structure on the curves of Fig. 2 at $L_1 \neq L_2$.

We show separately (Fig. 4) a plot of the depth of modulation of the critical-current curve

$$m=1-I_{min}^{(n)}/I_{max}^{(n)}, \tag{14}$$
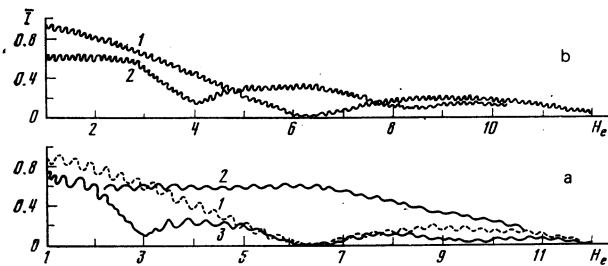

FIG. 3. Interference-type dependences of I on H_e for broad junctions: a—$\sigma=20$, curves 1—$L_1=L_2=1$, curves 2—L_1 $=0.01, L_2=0.5$, curves 3—$L_1=1, L_2=2$; b—$\sigma=50$, curves 1— $L_1=L_2=1$; curves 2—$L_1=0.5, L_2=1.5$.
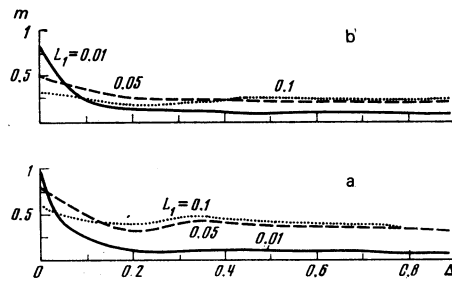

FIG. 4. Depth of modulation m of the plot of the maximum current as a function of the difference $\Delta=L_2-L_1$ of the junction widths: a—$\sigma=20$, b—$\sigma=50$.

where $I_{min}^{(n)}/I_{max}^{(n)}$ is the ratio of the values of the critical current in the neighboring minima and maxima. It is seen from Figs. 2–4 that the largest depth of modulation is a characteristic of symmetrical junction of small width ($L_1=L_2 \ll 1$).

In the limiting case of symmetrical point junctions it can be assumed that the field inside the interferometer coincides with the field on the outside ($H_0=H_e$). Equation (12) then yields the critical current $I_{max}=2H_{Imax}$:

$$I_{max}=2L \left| \cos \frac{\sigma H_e}{2} \right|, \tag{15}$$

which agrees with the result obtained earlier from simple physical considerations.[1,5] Equation (15) predicts for a symmetrical interferometer a maximum depth of modulation ($m=1$) and vanishing of the critical current at external-flux values $\phi_e=\sigma H_e=\pi n$.

We note that the assumption $H_0=H_e$ certainly does not hold in the case of non-symmetrical contacts, inasmuch as they carry, generally speaking, different currents and consequently a circular current flows around the ring and produces an additional flux inside the ring. For symmetrical junctions of finite width ($L_1=L_2=L$) we can likewise not assume that in the general case $H_0=H_e$, inasmuch as the Meissner effect produces in the system a screening current and therefore the fields inside and outside the ring differ. In the general case, as shown by calculations by means of the exact formula (12) (see Figs. 2–4), the depth of modulation differs from unity and the critical current vanishes nowhere. In this connection, the equations for $I_{max}(H_e)$, given, for example, in Ref. 1 and based on the assumption H_0 $=H_e$ (i.e., without allowance for the screening currents) give the correct dependence only in the case $L_1=L_2 \ll 1$.

4. In a number of theoretical papers (see Refs. 2 and 4 the literature cited therein) the critical current of a symmetrical interferometer was obtained with allowance for the screening current, using relations of the type

$$\phi_i=\phi_e-lj_{scr}, $$
$$j_{tot}=|j_1|+|j_2|, \quad j_{scr}=(|j_2|-|j_1|)/2, \tag{16}$$

where $j_1=\sin\varphi_1$ and $j_2=\sin\varphi_2$ are the dimensionless currents through junctions 1 and 2 of the interferometer (the junctions were assumed to be pointlike, since the phase shifts φ_1 and φ_2 assumed to be independent of the coordinates), l is a phenomenological self-inductance

parameter of the contour, and takes into account the decrease of the external flux through the interferometer ring (ϕ_e) because of the screening circulating current flowing around the ring (j_{scr}). The parameter 1 was not determined in this case, and the critical current was obtained from (16) numerically by choosing the optimal phase difference φ_1 (for details see Ref. 2).

It is easy to verify that our relations (8) in the case $L_1 = L_2 = L \ll 1$ can be represented in the form (16) by assuming the identity

$$l = \sigma L. \tag{17}$$

We shall show that the identity (17) is in fact satisfied in the general case and is a trivial consequence of the boundary conditions. Indeed, we have, [see (5), (11)]

$$\bar{j}_1 = \frac{1}{L} \int_0^L \sin \varphi_1 \, dx = \frac{H_e - H_0 - H_I}{L},$$

$$\bar{j}_2 = \frac{1}{L} \int_0^L \sin \varphi_2 \, dx = \frac{H_e - H_0 + H_I}{L}, \tag{18}$$

from which we get

$$H_0 = H_e - L(\bar{j}_1 + \bar{j}_2)/2. \tag{19}$$

Multiplying (19) by the area σ of the ring, we obtain the sought connection between the currents $\phi_i = \sigma H_0$ and $\phi_e = \sigma H_e$:

$$\phi_i = \phi_e - \sigma L \bar{j}_{scr}, \tag{20}$$

$$\bar{j}_{scr} = \frac{1}{2} (\overline{\sin \varphi_1} + \overline{\sin \varphi_2}), \quad \overline{\sin \varphi} = \frac{1}{L} \int_0^L \sin \varphi(x) \, dx. \tag{21}$$

Relation (20) at $L \ll 1$ (i.e., $\varphi_{1,2} = $ const) coincides with (16) if we define l with the aid of (17) and take into account the difference in the determination of the sign of φ_1. Thus, the self-induction coefficient of a symmetrical interferometer in the general case of arbitrary L, is equal (in dimensionless units) to the product of the ring area by the width of the junctions).

In dimensional units, the connection (21) between the external and internal fluxes can be represented in the form

$$\Phi_i = \Phi_e - \mathscr{L} I_{scr}, \quad I_{scr} = \frac{1}{2}(I_2 - |I_1|), \tag{22}$$

where Φ_i, Φ_e, and I_{scr} are respectively the total flux and the dimensional flux flowing around the ring; $\mathscr{L}$ is the dimensional self-induction coefficient which can be represented, taking footnote 1 into account, in the form

$$\mathscr{L} = \frac{\Phi_0}{2\pi} \frac{\pi r^2}{\lambda_J^2 \Lambda j_c}. \tag{23}$$

We note that Eqs. (17) and (23) for the self-inductance coefficient of a double interferometer coincide with the analogous equations obtained by us earlier for the self-inductance coefficient of a single ring interferometer.[7]

The results given by Solymar[2] coincide with our calculations at $L \ll 1$, if it is recognized that the parameter $2\pi \mathscr{L} I_J / \Phi_0$ used by Solymar coincides in dimensional units with our quantity l (17). A similar correspondence can be established also with the results given in the book of Likharev and Ul'rich.[4] We note that there is no

need to introduce explicitly the self-inductance coefficient l in our Eqs. (9)–(13), because the screening effects are already taken into account automatically via the geometrical parameters of the system L_1, L_2, and σ, and via the boundary conditions.

Thus, our general formulas (9)–(13) lead in the case of point junctions $L_1 = L_2 \ll 1$ to results known from the literature.[2,4]

5. Besides the critical current of the interferometer, it is useful to have information on the magnetic field H_0 that is established inside an interferometer placed in an external field H_e. This information can be obtained by solving (9) and (11) with respect to H_e. As a result we get

$$H_e = H_0 + \frac{H_I(s_2^2 - s_1^2) \pm R_I s_1 s_2 \sin \Sigma H_0}{s_1^2 + s_2^2 + 2s_1 s_2 \cos \Sigma H_0}, \tag{24}$$

where

$$R_I = (s_1^2 + s_2^2 + 2s_1 s_2 \cos \Sigma H_0 - 4H_I^2)^{1/2},$$

and s_1 and s_2 are defined in (10).

In the absence of a transport current ($H_I = 0$) we get from (24) the relation

$$H_e = H_0 \pm \frac{s_1 s_2 \sin \Sigma H_0}{\{s_1^2 + s_2^2 + 2s_1 s_2 \cos \Sigma H_0\}^{1/2}}, \tag{25}$$

which goes over for a symmetrical double interferometer ($L_1 = L_2 = L$) into the expression

$$H_e = H_0 \pm \varepsilon \frac{2}{H_0} \sin \frac{\Sigma H_0}{2} \sin \frac{L H_0}{2},$$

$$\varepsilon = \text{sign} \cos \frac{\Sigma H_0}{2}. \tag{26}$$

The last formula is analogous to the result

$$H_e = H_0 + \frac{2}{H_0} \sin \left[\left(\sigma + \frac{L}{2} \right) H_0 \right] \sin \frac{L H_0}{2}, \tag{27}$$

obtained by us[7] for the field inside a single ring interferometer with junction width L. A comparison of (26) and (27) shows that for the double interferometer the $H_e(H_0)$ curve has two branches [in accord with the two signs in (26)] in contrast to the single branch in (27) for a single interferometer. The presence of two branches of the function $H_e(H_0)$ was noted earlier in a paper by Matsinger et al.,[13] who considered the case of a double interferometer at $L_1 = L_2 = L \ll 1$.

Figures 5–7 show plots of $H_0(H_e)$ obtained from (24) at different values of L_1, L_2, σ, and H_I. Each point on these curves corresponds to a possible state of the system. (We note that the states of the system obtained from (24) and from Figs. 5–7 coincide with those obtained from (12).) At $H_I = 0$ and at finite $L_1 = L_2$ the curves show a beat pattern (we use a term from oscillation theory), analogous to the case of the single interferometer.[7] The cause of these beats is that the flux quantum, on penetrating into the interior of the system, need not necessarily enter immediately into the ring, and can become stuck inside the junction at finite $L_{1,2}$. At $L_1 \neq L_2$ there appear on the curves additional interference singularities connected with the addition of "oscillations" on different junctions (Figs. 5–7).
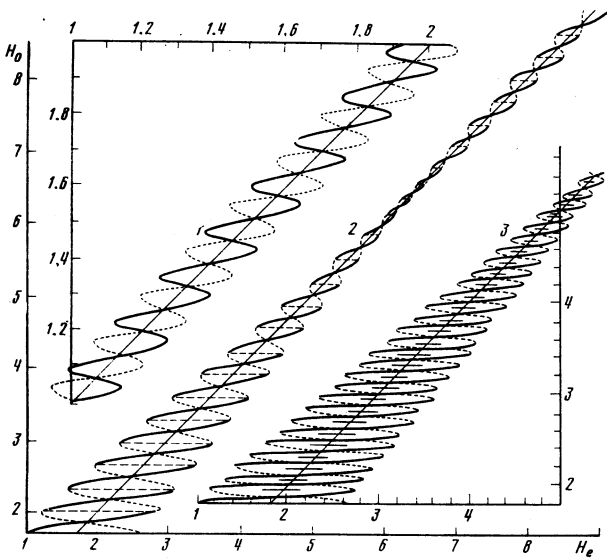
FIG. 5. Plot of $H_0(H_e)$ according to (24) at $H_I = 0$: 1—σ = 50, L_1 = 0.1, L_2 = 0.5; 2—σ = 20, $L_1 = L_2 = 1$; 3—$\sigma = 50, L_1 = L_2 = 1$.

We note that both branches of the $H_0(H_e)$ curves at H_I = 0 are continuous and for any H_e there are at least two static states with a certain value of an internal field H_0. With increasing parameters $L_{1,2}$ and σ, the number of such states increases. At $H_I \neq 0$ discontinuities appear on the $H_0(H_e)$ curves and are due to the fact that the radicand in (24) becomes negative and static states become impossible. At these values of H_e the interferometer goes over into a nonstationary condition.

6. The next step is the investigation of the stability of the states corresponding to the curves shown in Figs. 5 and 6. We start the stability investigation with non-stationary equations of the type (cf. Refs. 7–12)

$$\frac{d^2\varphi_i}{dt^2} + \beta\frac{d\varphi_i}{dt} - \frac{d^2\varphi}{dx^2} + \sin\varphi_i = 0 \quad (i = 1, 2), \tag{28}$$

which describe the time evolution of the solutions in
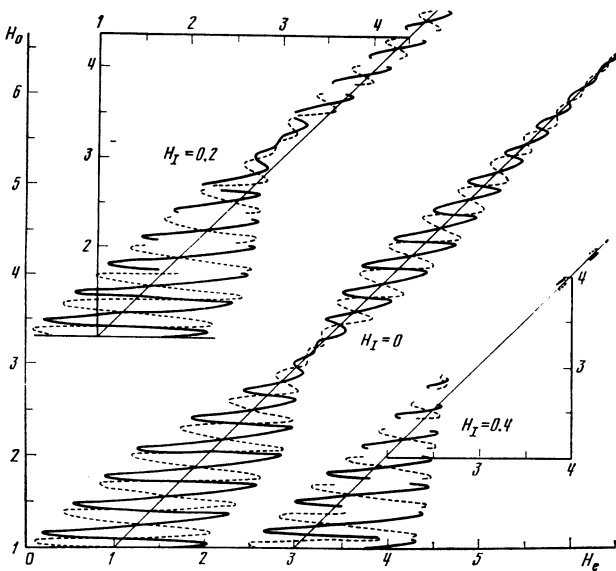

FIG. 6. Plot of $H_0(H_e)$ at $\sigma = 20$ for $L_1 = 1$, and $L_2 = 2$. The values of H_I are indicated on the curves.
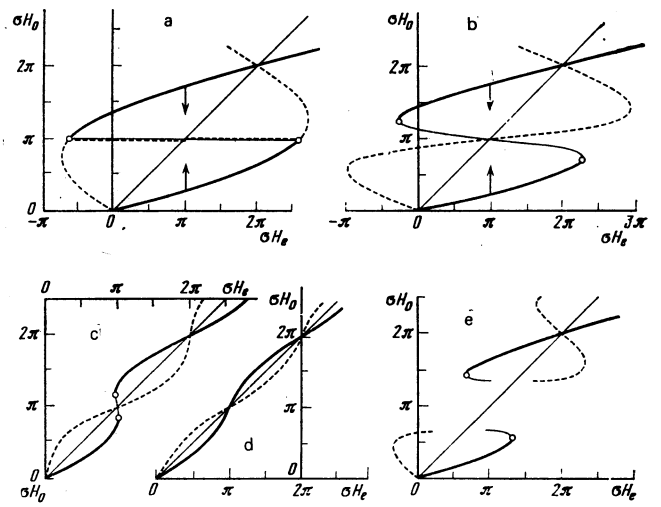

FIG. 7. Plot of $H_0(H_e)$ for point junctions at $H_I = 0, \sigma = 500$; a—$L_1 = L_2 = 0.01$; b—$L_1 = 0.01, L_2 = 0.02$; c—$L_1 = 0.002, L_2 = 0.01$; d—$L_1 = 0.001, L_2 = 0.01$; e—$L_1 = L_2 = 0.01$ at $H_I = 0.005$. Solid line—branch corresponding to the plus sign in (40), dashed—to the minus sign. The stable states are shown by thick lines and the stability boundaries ($E = 0$) are marked by circles. The points of equilibrium transition from branch to branch are marked in Figs. a and b by vertical arrows.

both junctions 1 and 2. Here β is a phenomenological parameter that takes into account the damping and ensures establishment of a static solution as $t \to \infty$. For simplicity we put $\beta_1 = \beta_2 = \beta$, assuming that the contact differ only in width. Writing

$$\varphi_i(x, t) = \varphi_i(x) + \psi_i(x)e^{\omega_i t}, \quad |\psi_i| \ll 1, \tag{29}$$

where $\psi_i(x)e^{\omega_i t}$ are the Fourier components of the small deviation from the investigated static solution $\varphi_i(x)$, we get from (28) the linearized equations

$$\frac{d^2\psi_i(x)}{dx^2} - \cos\varphi_i(x)\psi_i(x) = E_i\psi_i(x), \quad E_i = \omega_i^2 + \beta\omega_i. \tag{30}$$

The boundary conditions (5) take in this case the form

$$\frac{d\psi_1(x)}{dx}\Big|_{x=0} = \frac{d\psi_2(x)}{dx}\Big|_{x=0} = \frac{\psi_1(0) + \psi_2(0)}{\sigma}, \tag{31}$$

$$\frac{d\psi_1(x)}{dx}\Big|_{x=L_1} = \frac{d\psi_2(x)}{dx}\Big|_{x=L_2} = 0. \tag{32}$$

In (31) we must put $\omega_1 = \omega_2 = \omega$ and $E_1 = E_2 = E$, otherwise the boundary conditions (5) cannot be satisfied at all instants of time. The system (30) with the boundary conditions (31) and (32) makes it possible to find the spectrum of the eigenvalues ω (or E). If some of them are positive ($\omega > 0$), then the deviations $\psi_{1,2}(x)e^{\omega t}$ will increase with time and the investigated static solutions $\varphi_{1,2}(x)$ will be unstable. On the other hand, if all the eigenvalues are negative, then the deviations $\psi_{1,2}e^{\omega t}$ will attenuate with time and the solutions $\varphi_{1,2}(x)$ will be stable.

We determine the spectrum of the eigenvalues ω for the simple case $L_{1,2} \ll 1$, when the phase shifts $\varphi_{1,2}$ can be regarded as independent of the coordinates. Equations (30) then take the form

$$\frac{d^2\psi_i(x)}{dx^2} = \varepsilon_i\psi_i(x), \quad \varepsilon_i = E + \cos\varphi_i, \tag{33}$$

$$E = \omega^2 + \beta\omega. \tag{34}$$

The solutions of these equations can be easily written down (with allowance for the fact that ε_i is constant):

$$\psi_i = a_i \exp(\varepsilon_i^{1/2} x) + b_i \exp(-\varepsilon_i^{1/2} x). \tag{35}$$

The boundary conditions (31) and (32) reduce to a system of four linear homogeneous equations whose determinant gives the dispersion relation (at $L_{1,2} \ll 1$)

$$\sigma\varepsilon_1\varepsilon_2 L_1 L_2 + \varepsilon_1 L_1 + \varepsilon_2 L_2 = 0, \quad \varepsilon_{1,2} = E + \cos\varphi_{1,2}. \tag{36}$$

Solving the quadratic equation (36) we obtain the spectrum of E:

$$E = -\frac{1}{2}\left(\cos\varphi_1 + \cos\varphi_2 + \frac{1}{\sigma L_1} + \frac{1}{\sigma L_2}\right) + R \quad (R > 0),$$

$$R = \left\{ \frac{(\cos\varphi_1 - \cos\varphi_2)^2}{4} + \frac{1}{4}\left(\frac{1}{\sigma L_1} + \frac{1}{\sigma L_2}\right)^2 \right. \tag{37}$$

$$\left. + \frac{\cos\varphi_1}{2}\left(\frac{1}{\sigma L_1} - \frac{1}{\sigma L_2}\right) + \frac{\cos\varphi_2}{2}\left(\frac{1}{\sigma L_2} - \frac{1}{\sigma L_1}\right) \right\}^{1/2}.$$

In (37) it suffices to retain the plus sign in front of the square root R, since we are interested only in the presence of positive values of E.

The growth rates of the solutions obtained from (34):

$$\omega = -\frac{1}{2}\beta \pm (\frac{1}{4}\beta + E)^{1/2}, \quad \beta > 0. \tag{38}$$

If $E > 0$, then there must exist a positive root $\omega > 0$ and the solution is unstable. If all the $E < 0$, then $\omega < 0$ and the solution is stable. The value $E = 0$ corresponds to the stability threshold.

We write down also the conditions (8) in the case

$$H_c - H_0 = L_1 \sin\varphi_1, \quad H_e - H_0 = L_2 \sin\varphi_2,$$

$$\varphi_2 = \sigma H_0 - \varphi_1 \tag{39}$$

and Eq. (27), which now takes the form

$$H_e - H_0 = \pm \frac{L_1 L_2 \sin\sigma H_0}{\{L_1^2 + L_2^2 + 2L_1 L_2 \cos\sigma H_0\}^{1/2}}. \tag{40}$$

The determination of the stability of the state reduces thus to the following operations. We first specify a certain value H_0 and obtain from (40) the position of the representative point on the $H_0(H_e)$ curves. We then obtain from (39) the values of φ_1 and φ_2, and from (37) we determine the value of E and its sign, which gives the stability criterion of the investigated state.

Figure 7 shows, in magnified scale, the plots obtained from (40) in the periodicity interval $0 \le \sigma H_0 \le 2\pi$. The solid line indicates the branch corresponding to the plus sign in (40), the thick lines indicate the stable states, and the circles mark the points where $E = 0$. The dashed line corresponds to the branch with minus sign in (40), and all the states on this branch are unstable.

Figure 8 shows the values of the phase shifts $\varphi_1^{\pm}$ and $\varphi_2^{\pm}$ as functions of the field H_0, obtained from (39) for the two branches corresponding to the $\pm$ signs in (40).

In the case $L_1 = L_2 = L$, Eq. (40) takes the simpler form[3]

$$H_c - H_0 = \pm \varepsilon L \sin(\sigma H_0/2), \quad \varepsilon = \text{sign} \cos(\sigma H_0/2), \tag{41}$$
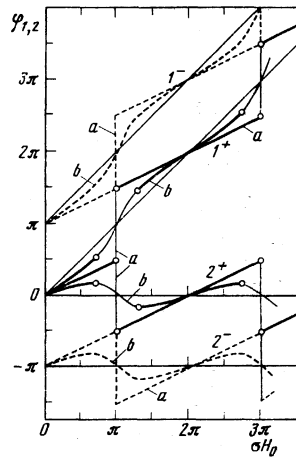
and from (39) it now follows that

$$\varphi_1^+ = \frac{1}{2}\sigma H_0 + 2\pi n$$
$$\varphi_2^+ = \frac{1}{2}\sigma H_0 - 2\pi n$$

for the branch with the plus sign in (40) and

$$\varphi_1^- = \frac{1}{2}\sigma H_0 + \pi + 2\pi n,$$
$$\varphi_2^- = \frac{1}{2}\sigma H_0 - \pi - 2\pi n$$

for the branch with the minus sign. Expression (37) for E also takes on the simple form

$$E = -\cos\varphi, \quad \varphi = \sigma H_0/2. \tag{42}$$

The stability threshold ($E = 0$) corresponds in this case to $\cos\varphi = 0$ (i.e., $\sigma H_0 = (2n + 1)\pi$), which coincides with the criterion obtained in Ref. 13 by another method for a symmetrical interferometer.

If the junctions differ greatly in width (for example, $L_1 \ll L_2 \ll 1$), then we get from (40)

$$H_e - H_0 = \pm L_1 \sin\sigma H_0. \tag{43}$$

We see therefore that the properties of the double strongly asymmetrical interferometer are determined entirely by the weakest link (L_1), and the stable branch (43) (with the plus sign) coincides with the relation $H_e - H_0 = L \sin\sigma H_0$ for a single interferometer [formula (27) at $L \ll 1$]. This means that the behavior of a strongly asymmetrical double interferometer in an external field (at $H_I = 0$) is the same as that of a single interferometer with $L = L_1$ (see Figs. 7c, d). In particular, there are no hysteresis states (see below) at $\sigma L_1 < 1$ in an asymmetrical double interferometer (Fig. 7e), just as for the single interferometer. It is also easy to show that the stability criterion (37) (at $L \to 0$, $\varphi_2 \to 0$, $\varphi_1 \to \sigma H_0$, see Fig. 8) yields $E = 0$ at the points $\cos\sigma H_0 = -1/\sigma L_1$, which coincides with the stability criterion for a single interferometer.[7,13]

7. An examination of the curves shown in Figs. 5-7 indicates that in a given external field H_e a double interferometer can have in the general case several stable states. This points to the possibility of a hysteresis behavior of the interferometer in an external field (cf. Ref. 13). If the representative point of the state lies on stable branch, then with increasing H_e, when the stabili-

ty boundary is reached (points marked by circles in Fig. 7), the solution must jump over to the higher-lying stable branch.[4] When H_e is subsequently decreased, the representative point moves along the higher branch until it again reaches the stability boundary, where it must go over to the lower branch. Thus, the stability-loss points determine the boundaries of the possible hysteresis behavior (the limits of the "superheating" and "supercooling" in the magnetic field, cf. Ref. 14). Under real conditions, the jumps from branch to branch need not coincide with the stability-loss points, and can occur earlier, for example at points where the free energies of the corresponding states become equal (the equilibrium-transition points). To find the points of the equilibrium transition it is necessary to know the free energy of the system.

The expression for the free energy G of a double interferometer can be easily obtained by a method used by us earlier in the case of a single ring interferometer (cf. Refs. 7, 15). From the mathematical point of view the solution of the boundary problem (1), (5), (6) is an extremal of the functional G, i.e., the condition $\delta G = 0$ must be satisfied on the solution at fixed boundary conditions. Taking this into account we easily obtain

$$G = \mathscr{E}_1[\varphi_1] + \mathscr{E}_2[\varphi_2] + (\varphi_1(0) + \varphi_2(0))^2/2\sigma - (H_{L1}\varphi_1(L_1) + H_{L2}\varphi_2(L_2)). \quad (44)$$

Here $\mathscr{E}_1$ and $\mathscr{E}_2$ are the energies of weak superconductors[1,2]

$$\mathscr{E}_1[\varphi_1] = \int_0^{L_1} \left[\frac{1}{2}\left(\frac{d\varphi_1}{dx}\right)^2 + 1 - \cos\varphi_1 \right] dx,$$

$$\mathscr{E}_2[\varphi_2] = \int_0^{L_2} \left[\frac{1}{2}\left(\frac{d\varphi_2}{dx}\right)^2 + 1 - \cos\varphi_2 \right] dx. \quad (45)$$

The third term in (44) can be written, when (6) is taken into account, in the form $\sigma H_0^2/2$, i.e., it constitutes the energy of the magnetic field in the cavity ($\sigma_0^2/8\pi$ in dimensional units), while the last term in (44) is interpreted as the flux of the Poynting vector through the edges of the junctions into the interior of the system.[5] With the aid of (44) and (45) we can calculate the free energy of the system, if we know the solutions $\varphi_1(x)$ and $\varphi_2(x)$ for both junctions [we recall that the solution (x) is determined completely by the values of $\varphi(0)$ and $d\varphi/dx|_{x=0}$]. In the case of point junctions and at $H_I = 0$, the expression for G takes the simpler form

$$G = L_1(1 - \cos\varphi_{10}) + L_2(1 - \cos\varphi_{20}) + \sigma H_0^2/2 - H_e\sigma H_0 + H_0^2(L_1 + L_2)/2. \quad (46)$$

The positions of the points of the equilibrium transition, where the free energies of the states corresponding to the lower and upper curves of Fig. 7a and b become equalized, are shown on these figures by vertical arrows.

We have thus demonstrated above that, within the framework of the assumed model, it is possible to describe completely the behavior of a double interferometer, namely, to find, given the external field, both the internal field and the configuration of the fields and currents in both junctions,[6] to determine the entire spectrum of the possible states (both stable and unstable), to find the limits of the hysteresis behavior and the

points of equilibrium transition between the states, and to determine the function $I_{max}(H_e)$ for an asymmetrical interferometer. The derived equations can be compared directly with experiment. The results obtained above are valid formally at $H_e \gg 1$, but it can be shown that for point junctions ($L_{1,2} \ll 1$) these formulas are suitable also for arbitrary fields. In the case of junctions of finite width in fields $H_e \lesssim 1$, deviations from the simple equations such as (12) and (24) appear, and the oscillatory curves (Figs. 2–7) assume a more complicated nonlinear form. To find these curves in weak fields it is necessary to turn to the exact equations (3)–(6) and find the values of φ_{01}, φ_{02}, and H_0 with the aid of rather cumbersome numerical calculations (cf. the similar problem considered in Ref. 7).

---

[1] We use dimensionless variables, with the lengths measured in units of λ_J (the Josephson depth of penetration, $\lambda_J \sim 0.1$ mm), the current is measured in units of j_c (the maximum density of the stationary current through the barrier), the field is measured in units of $H_J = \Phi_0/2\pi\lambda_J\Lambda \sim 1$ G (where Φ_0 is the flux quantum, $\Lambda = 2\lambda_L + t$, λ_L is the London depth, and $t \sim 10^{-7}$ is the thickness of the dielectric liner of the barrier), the flux is measured in units of $\Phi_0/2\pi$ and the dimensionless area is $\sigma = S/\lambda_J\Lambda$.

[2] The plus sign in (6) is the result of the fact that on going around the cavity σ in a counterclockwise direction we reckon the phase difference between the upper and lower edges of the cuts L_1 and L_2 respectively along the contour. A relation of the type (6) is usually written with φ_{01} taken with a minus sign, corresponding to a different definition of the phase difference.

[3] We note that Eq. (41) is analogous to Eq. (18) of Ref. 13 (the correspondence can be observed by multiplying our Eq. (41) by σ and introducing the inductance $l \equiv \sigma L$. However, (41) contains an additional sign factor ε, which reflects the continuity of both branches of the $H_0(H_e)$ curves (see Figs. 7a, b). In Ref. 13 the horizontal sections of the branches on Fig. 7a were not taken into consideration, therefore the authors arrived at the incorrect conclusion that in a double symmetrical interferometer the oscillations of the field $H_0(H_e)$ are half as frequent as in a single interferometer. In fact, as is obvious from Fig. 7, the number of zeros of the functions $H_0(H_e)$ is the same for both interferometers.

[4] In fact, the jump has a dynamic character—when the stability boundary is reached a restructuring of the flip configuration and of the current takes place within a time $\tau \sim 10^{-10}$ sec. Examples of solutions of dynamic problems of this kind are given in Refs. 9–11.

[5] Recognizing that $E = d\varphi/dt$ is the electric field intensity in the junction, we can respresent the pointing vector $S = EH$ in the form $S = H_L d\varphi/dt$. Integrating this expression with respect to time, we obtain the contribution $-H_L\varphi(L)$ for the energy that flows in through the edge of the junction into the interior of the system.

[6] To determine these configurations we must find the quantity H_0 and then obtain from (6)–(8) the values of φ_{01} and φ_{02}. The "initial" values φ_{01}, φ_{02}, and $H_0 = d\varphi_{1,2}/dx|_{x=0}$ determine completely the solutions of Eqs. (1) and the corresponding configurations of the field and of the current in the junctions. In explicit form the solution of Eqs. (1) for the case $H_e \gg 1$ is given in Ref. 12.

110   Sov. Phys. JETP 51(1), Jan. 1980

G. F. Zharkov and A. D. Zaikin   110

[1]I. O. Kulik and I. I. Yanson, Effekt Dzhozefsona v sverkhpro-vodyashchikh tunnel'nykh strukturakh (Josephson Effect in Superconducting Tunnel Structures), Nauka, 1970.

[2]L. Solymar, Superconductive Tunneling and Applications, Wiley, 1972.

[3]O. V. Lounasmaa, Experimental Principles and Methods below 1 K, Academic, 1974.

[4]K. K. Likharev and B. T. Ul'rikh, Sistemy s dzhozefsonov-skimi kontaktami (Systems with Josephson Junctions), Moscow Univ. Press, 1978.

[5]R. C. Jaklevich, J. Lambe, J. E. Mercereau, and A. H. Silver, Phys. Rev. Lett. 12, 274 (1964).

[6]R. C. Jaklevich, J. Lambe, J. E. Mercereau, and A. H. Silver, Phys. Rev. 140, A 1628 (1965).

[7]G. F. Zharkov and A. D. Zaikin, Zh. Eksp. Teor. Fiz. 77, 223 (1979) [Sov. Phys. JETP 50, 114 (1979)].

[8]G. F. Zharkov, ibid. 71, 1951 (1976) [44, 1023 (1976)].

[9]G. F. Zharkov and S. A. Vasenko, ibid. 74, 665 (1978) [41, 350 (1978)].

[10]S. A. Vasenko and G. F. Zharkov, ibid. 75, 180 (1978) [48, 89 (1978)].

[11]G. F. Zharkov and A. D. Zaikin, Fiz. Nizk. Temp. 4, 586 (1978) [Sov. J. Low Temp. Phys. 4, 283 (1978)].

[12]G. F. Zharkov, Zh. Eksp. Teor. Fiz. 75, 296 (1978) [Sov. Phys. JETP 48, 1107 (1978)].

[13]A. A. J. Matsinger, R. de Bruyn Ouboter, and H. van Beelen, Physica 94B, 91 (1978).

[14]V. L. Ginzburg, Usp. Fiz. Nauk 42, 169, 133 (1950).

[15]G. F. Zharkov and A. D. Zaikin, Kratkie soobshcheniya po fizike (FIAN SSSR) No. 7, 21 (1978).

Translated by J. G. Adashko

Theory of pure short S–c–S and S–c–N microjunctions

A. V. Zaĭtsev

(Submitted 11 July 1979)
Zh. Eksp. Teor. Fiz. 78, 221–233 (January 1980)

A theory is developed for the nonstationary Josephson effect in pure S–c–S junctions (mean free path l much larger than the constriction radius a), and the current-voltage characteristic (CVC) of such a junction is obtained. The model considered for the construction was an opening of small radius $a \ll (\xi^{-1}(0) + l^{-1})^{-1}$ in a thin impermeable partition [Kulik and Omel'yanchuk, Sov. J. Low Temp. Phys. 3, 459 (1977); Omel'yanchuk, Kulik, and Shekhter, JETP Lett. 25, 437 (1977)]. A linear response from an S–c–S junction was obtained with a direct current smaller than the critical value, and the resistive regime was investigated in the voltage region $V \ll \Delta$ near T_c and in the region $V \gg \Delta$ at arbitrary temperatures. In the case of the S–c–N junction, the CVC was obtained for arbitrary V and T. The results differ not only quantitatively but also qualitatively from those obtained by Artemenko, Volkov, and Zaĭtsev [Soviet Phys. JETP 49, 924 (1979); Solid State Commun. 30, 771 (1979)] for dirty short constrictions.

PACS numbers: 74.50. + v, 73.40.Gk

INTRODUCTION

It is known that weakly coupled structures of the S–c–S type (S—superconductor, c—geometrical constriction), which include point contacts, junctions of variable thickness, etc., are the most promising for applications.[1] Although much progress was made recently in the study of the properties of such systems, the results were obtained for the so-called "dirty" constrictions, i.e., those whose characteristic dimensions a and d (which characterize the respective parameters of the constriction in the plane normal to the current direction and in the same direction) greatly exceed the mean free path l.

The study of the Josephson effect in S–c–S was initiated by Aslamazov and Larkin.[2] It is based on the simplified nonstationary Ginzburg–Landau equations, which are generally speaking valid only for zero-gap superconductors. They have shown[2] that near T_c the Josephson effect in short dirty constrictions $(l \ll (a,d) \ll \xi T)$ can be described within the framework of a simple resistive model, in which the current is the sum of an ohmic component and a Josephson component:

$$I = V(t)/R + I_c \sin \varphi, \quad V(t) = \dot{\varphi}/2, \qquad (1)$$

where φ is the phase difference of the order parameter and $V(t)$ is the voltage on the junction (the electron charge is assumed equal to unity). It follows from (1) that the current–voltage characteristic (CVC), which is the dependence of the time-averaged voltage V on the direct current, is of the form

$$V = R(I^2 - I_c^2)^{1/2}. \qquad (2)$$

In experiment, however, deviations are observed from the resistive model; this is not surprising, since the latter was obtained on the basis of simplified equations. In recent studies of the properties of S–c–S systems, microscopic equations have been used. Kulik and Omel'yanchuk[3], using the Eulenberger equations that describe equilibrium processes in superconductors, have constructed the theory of the stationary Josephson effect in short dirty microjunctions, where the following condition is valid:

$$l \ll (a, d) \ll (D/\Delta)^{1/2}. \qquad (3)$$

Here $D = l v_F/3$ is the diffusion coefficient. It turned out that the connection between the current and the phase difference deviates from the Josephson relation when